Lunar X-ray Imaging Spectrometer (*LuXIS*): A 2020 Decadal Survey White Paper

Jaesub Hong[1*], Suzanne Romaine[2], Larry Nittler[3], Martin Elvis[2], Ian Crawford[4], Graziella Branduardi-Raymont[5], Lucy Rim[6], Scott Wolk[2]

[1] *Harvard University*, [2] *Smithsonian Astrophysical Observatory*, [3] *Carnegie Institution of Washington*, [4] *Birbeck College, University of London, UK*, [5] *University College London, UK*, [6] *NASA Goddard Space Flight Center*, **Corresponding author: jhong@cfa.harvard.edu*

A Mission Concept White Paper submitted to the *The Planetary Science and Astrobiology Decadal Survey 2023-2032* Committee, National Academies of Sciences, Engineering and Medicine
August 15, 2020

Lunar X-ray Imaging Spectrometer (LuXIS) is a SmallSat mission that advances our understanding of the Moon's origin and evolution through measuring elemental abundances of multiple lunar surface regions of specific geological interest with high spatial resolution. Based around miniature focusing X-ray optics and radiation tolerant CMOS X-ray sensors, *LuXIS* uses the method of X-ray fluorescence to determine the abundances of key rock-forming elements including Mg, Al, Si, and Fe. With reasonable measurement times, these can distinguish important sources and processes in lunar origin and evolution. *LuXIS* also serves as a pathfinder for autonomous precision deep-space navigation using X-ray pulsars.

1 Introduction

A planetary body's bulk elemental composition is set by its formation conditions and source materials, while geological processes such as differentiation and volcanism segregate the elements into different reservoirs (e.g., primary and secondary crusts, mantle, and core). Compositional measurements are thus crucial for investigating the origin and geological evolution of the Moon and other planetary bodies. Remote-sensing X-ray fluorescence (XRF) is a proven method for determining surface abundances of rocky worlds in the inner solar system (Hong et al., 2020). XRF lines, triggered either by solar X-rays or energetic ions, have characteristic energies intrinsic to atomic energy levels and carry an unambiguous signature of the elemental composition of the emitting bodies. Except for H, He and Li, all the atomic elements including life-essential (e.g., C, N, and O) and rock-forming elements (e.g., Mg, Al, Si, S, Ca, Ti, Cr, and Fe) are identifiable by their K, L or M shell XRF lines in the 0.1 to 15 keV band.

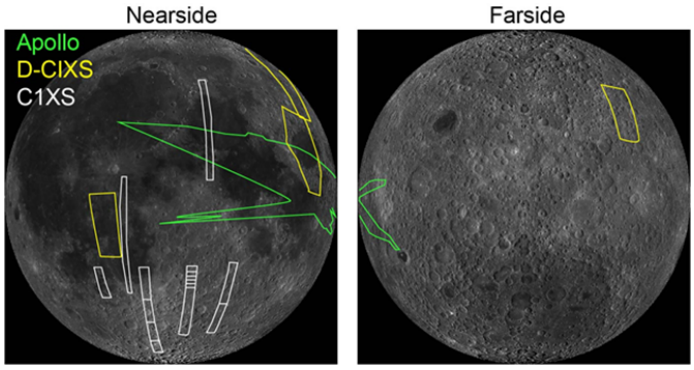

Figure 1: *Lunar regions investigated by previous XRF mapping missions outlined on LRO (Vondrak et al., 2010) Camera lunar basemap in orthographic projection. Spatial resolution of these data is larger than ∼30 km. Almost all of the sparse previous coverage is on the nearside.*

The Moon was the first target for remote-sensing XRF measurements, on *Apollo* 15 and 16 (Adler et al., 1972) and several subsequent missions have carried X-ray instruments for measuring the surface elemental composition of the Moon, with mixed success (e.g., Grande et al., 2009). Despite the proximity to Earth, the spatial coverage of all lunar XRF experiments to date is quite sparse and of relatively poor spatial resolution ($\gtrsim$30 km) as illustrated in Figure 1, due in part to the use of collimated instruments.

Global elemental abundance maps (e.g., K, Th, Fe, Ti) of the Moon, produced from remote-sensing γ-ray, neutron, and reflectance spectroscopy data, have been extremely useful for understanding the Moon's history. However, XRF spectroscopy extends measurements to geochemically highly important elements like Mg and Al, and the promise of higher-resolution measurements enabled by focusing X-ray optics will help to address multiple important science questions (next section).

Focusing X-ray optics provide true spectroscopic imaging and are used widely in astrophysics missions, but until now their mass and volume have been too large for resource-limited *in-situ* planetary missions. Recent advances in X-ray instrumentation such as the Micro-Pore Optics used on the *BepiColombo* X-ray instrument (Fraser et al., 2010), Miniature X-ray Optics (MiXO, Hong et al., 2016; Kashyap et al., 2020) and highly radiation tolerant CMOS X-ray sensors (e.g., Kenter et al., 2012) enable compact and lightweight, yet powerful, truly focusing X-ray Imaging Spectrometers. We describe here a mission concept called Lunar X-ray Imaging Spectrometer (*LuXIS*). *LuXIS*, formerly known as *CubeX*, is a MiXO-telescope-based lunar mission, whose concept was studied with support from NASA's Planetary Science Deep Space SmallSat Studies (PSDS3) program (Hong et al., 2018; Stupl et al., 2018). *LuXIS* is a SmallSat with a compact, highly radiation-tolerant, focusing X-ray telescope that identifies and spatially maps lunar crust and mantle materials excavated by impact craters, and also serves as a pathfinder for autonomous precision deep-space navigation using X-ray pulsars.

2 Science Objectives

The Moon contains a rich geological record of the inner Solar System, including clues to the origin and evolution of the Earth-Moon system (Jolliff et al., 2006). Lunar sample and meteorite analyses and remote sensing data have led to a paradigm that very early in its history the Moon experienced a stage of large-scale melting, known as the "**lunar magma ocean**" or **LMO**, which led to differentiation of the mantle and formation of a crust with a diverse range of lithologies (e.g., the feldspar-rich lunar highlands that formed by flotation on the LMO and the mare basalts which formed by partial melting of differentiated mantle material) (Wood et al., 1970a,b; Wood, 1970; Smith et al., 1970). However, a number of fundamental questions remain about the composition of the lunar crust and mantle and changes in composition as a function of depth in the crust. These compositional changes are thought to occur as a result of differentiation in the lunar crust during its formation (Elardo et al., 2011; Papike et al., 1991; Warren, 2001). *LuXIS* directly

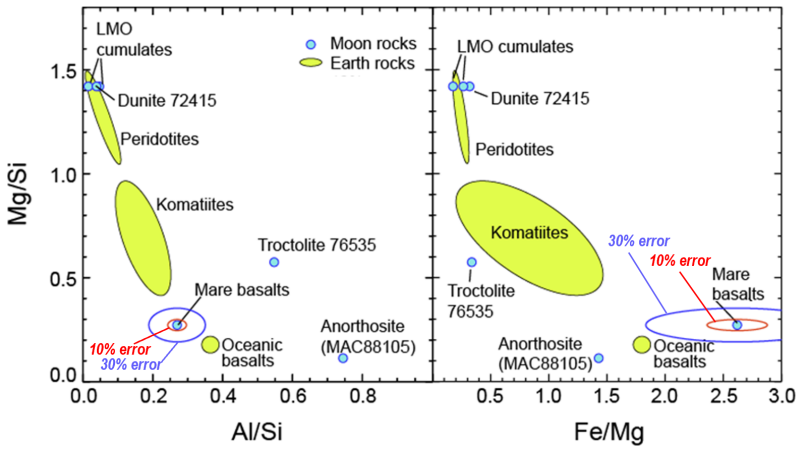

Figure 2: *LuXIS measures Mg/Si, Al/Si, Fe/Mg and other elemental ratios with relative precision ranging from 5% on a 100 km scale to 30% on a 3 km scale (e.g., blue ellipses) at C1 solar states, sufficient to distinguish diverse lunar compositions. LMO cumulates are predicted to have compositions of olivine-rich cumulates during LMO crystallization (Elardo et al., 2011). These olivine-rich cumulates may, after mantle overturn, be present in the Moon's present-day upper mantle. Lunar meteorite MAC88105 is representative of feldspar-rich lunar highlands rocks. Other plotted lunar compositions are rocks returned by Apollo missions.*

measures key elements at the lunar surface in order to compare measured values with samples and calculated trends in models of crustal formation as illustrated in Figure 2. The expected precision of the relative abundances measured by *LuXIS* ranges from 5% (systematics limited) at a 100 km scale or 10% at a 10 km scale, to 30% (statistics limited) at a 3 km scale, which are sufficient to distinguish diverse lunar compositions associated with the morphological features.

Objective 1: Measure the vertical and regional composition variation of the lunar crust by determining the compositions of crater central peaks, basin peak-rings, and ejecta blankets from a wide range of crater sizes ($\sim$10$-$200 km; e.g., Figure 3). Compositional measurements of the ejecta around 10–200 km size craters probe the vertical structure of the lunar crust to depths between 1 and 20 km since impact craters excavate material from depths approximately one-tenth of their diameter. For relatively large impact basins, central peaks and peak rings emerge from beneath excavation zones with depths roughly one-tenth of their transient crater diameter ($\sim$ half of the final crater diameter). Therefore, central peaks and peak rings may expose material from mid-crustal to upper mantle depths (Lemelin et al., 2015; Kring et al., 2016).

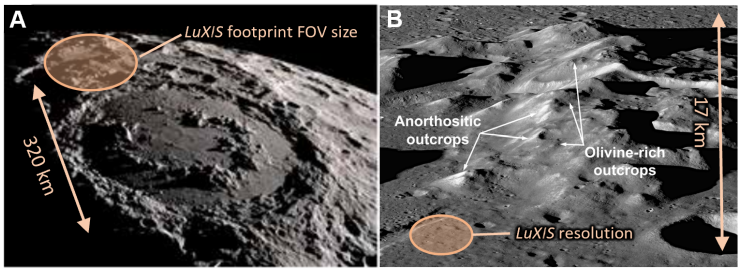

Figure 3: *(A) The morphology of a peak ring is evident in this view of the 320-km-diameter Schrödinger basin on the Moon, looking from the north toward the south pole (NASA's Scientific Visualization Studio). (B) A close-up view of a segment of the peak ring with rocks uplifted from mid- to lower-crustal levels by the impact event. The field of view is 17 km wide through the center of the image. LRO Camera image M1192453566 (Kring et al., 2016, 2017). Anorthositic outcrops are generally considered to be from highlands, whereas olivine-rich outcrops are associated with the mantle or lower crust origin.*

For the first time in a targeted approach, informed by developments over the past decades (e.g., *GRAIL, LRO*), *LuXIS* decisively characterizes the bulk elemental composition of the lunar surface in order to better define trends within the lunar crust. While the *Apollo* XRS data clearly showed variations within the crust, the spatial extent of the measurements is limited (Figure 1) (Adler et al., 1975; Clark & Hawke, 1982). Targeting a range of crustal thickness ($\sim$2$-$30 km) based on both the *GRAIL* data and crater sizes, *LuXIS* characterizes composition as a function of crustal thickness specifically for the abundances of Si, Al, and Mg (Taylor & Wieczorek, 2014). These elements are particularly sensitive tracers to variations due to differentiation at the time of crustal formation (Papike et al., 1991). Given the high-quality LROC imagery data we currently have of the Moon, we can place any measurement by *LuXIS* into a local and regional context that allows us to infer its crustal setting (Corley et al., 2018; Jolliff et al., 2011). The work of Taylor and Wieczorek (Taylor & Wieczorek, 2014) shows that the *GRAIL* data can be used in concert with elemental abundances from *Lunar Prospector* (Lawrence, 1998). *LuXIS* allows us to extend these analyses to other elements in an assessment of the bulk composition of the lunar crust.

Objective 2: Identify outcrops of lunar mantle on the surface (e.g., through high

Mg/Si), which then become possible targets for future sample return missions. Models of the Moon's formation depend heavily on the bulk chemical and isotopic composition of terrestrial and lunar mantle rocks (Armytage et al., 2012), but to date, no samples of the lunar mantle have been unambiguously identified. Some olivine-rich samples in the *Apollo* collection (e.g., dunite in Figure 2) have been suggested to be mantle xenoliths, but this is not widely accepted (Shearer et al., 2015).

LuXIS measurements are used to test the hypothesis that olivine at the lunar surface represents deep crustal or even mantle exposures (cf Yamamoto et al., 2010; Kring et al., 2016; Corley et al., 2018). *LuXIS* leverages knowledge of lunar mineralogy (Kramer et al., 2013; Yamamoto et al., 2010, 2012) and crustal thickness (Wieczorek et al., 2012) by targeting areas with known compositions or gravity signatures suggestive of lower crustal compositions or thin crust. *Lunar Prospector*'s measurements showed an inverse relationship between elevation and Fe content, suggesting a compositional trend due to a differentiated crust (Lawrence et al., 2002). *LuXIS* can investigate Mg and Al stratigraphy within the crust and upper mantle in addition to Fe.

Crustal thickness maps derived from *GRAIL* suggest there are no extensive regions of mantle exposures on the lunar surface, only areas with extremely thin crust (<5 km thick) most commonly associated with the interiors of impact basins. However, olivine exposures are known to be in areas of thin crust (Kramer et al., 2011; Yamamoto et al., 2010). With these locations as a guide, *LuXIS* measures the diagnostic relative abundances of Fe, Mg, Al, and Si (Figure 2) and tests the hypothesis that not all olivine exposures are representative of the mantle (Melosh et al., 2014). *LuXIS* measurements of Mg and Fe in particular are used to investigate suspected areas of mantle exposure (i.e., the interior of the South Pole-Aitken (SPA) Basin) as a function of the *GRAIL* crustal thickness. *LuXIS*'s identification of mantle outcrops assists in site selection for future sample return missions (e.g., *Resource Prospector*) and provides context of the sample over a large region surrounding the site (e.g., Schrödinger and SPA Basins).

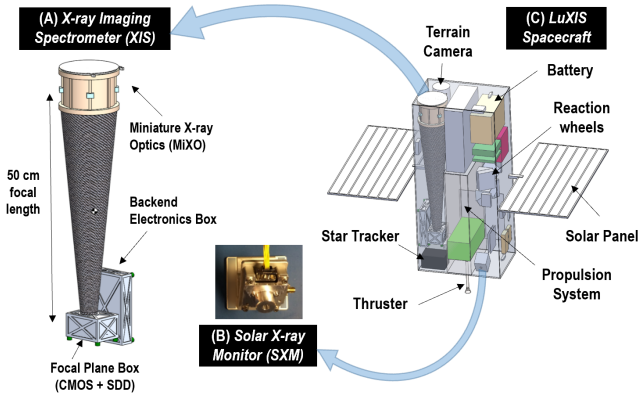

Figure 4: *Two instruments onboard LuXIS: (A) X-ray Imaging Spectrometer (XIS) and (B) Solar X- ray Monitor (SXM) w.r.t. (C) the LuXIS S/C. The SXM picture (not to scale) shows an actual flight model of OSIRIS-Rex/REXIS. The SXM location and its large FOV (130 deg FWZI) are optimized for Sun viewing. Both instruments share the same electronics box.*

3 Instrument Overview

LuXIS carries two X-ray instruments: an X-ray Imaging Spectrometer (XIS) and a Solar X-ray Monitor (SXM) as shown in Figure 4 and Table 1. The XIS is a focusing X-ray telescope in a small form factor. It is mainly designed to perform XRF imaging spectroscopy of the lunar

surface but also to be capable of technology demonstration for X-ray pulsar timing based navigation (XNAV) (Reichley et al., 1971; Downs, 1974; Chester & Butman, 1981) through precise X-ray time series measurements of millisecond pulsars (MSPs) without moving parts. Its focal plane combines two CMOS X-ray sensors for XRF imaging spectroscopy and a Silicon Drift Detector (SDD) with sub-microsecond timing resolution needed for XNAV operations. The SXM is a separate SDD with a filter in a small enclosure, designed to monitor the solar X-ray flux and its spectral evolution during XRF measurements of the lunar surface. When the XIS observes the Moon, the SXM simultaneously monitors the incoming solar X-ray flux, in order to later deconvolve the elemental abundance from the lunar XRF spectra. *LuXIS* also carries a terrain camera (TC), which takes optical images of target regions for precise spatial registration of X-ray images captured by the XIS. The SXM and the TC are operational during XIS observations of the lunar surface. *LuXIS* tests the XNAV performance in a more realistic environment for deep space travel, naturally extending what Neutron Star Interior Composition Explorer (*NICER*) on the International Space Station demonstrated (Winternitz et al., 2016; Witze, 2018). If the XNAV experiment is successful, versions of XIS could provide a practical autonomous navigation system for deep space missions.

Table 1: *Key XIS and SXM parameters*

Parameters	**XIS**	**SXM**
Main Subsystems	MiXO + 2 CMOS for XRF + 1 SDD for XNAV	Filter + 1 SDD
Mass	5.5 kg	0.3 kg
Volume	$\sim 10 \times 10 \times 60$ cm	$\sim 5 \times 5 \times 3$ cm
Power	8.6W (12.4W peak)	
Data	1.6 GB for 1 yr, 4−7 MB/day	
Focal length	50 cm	N/A
Ang. Res.	$<$ 1 arcmin ($<$ 3 km)	N/A
FOV (footprint)	$>$ 1 deg^2 (110 km)	$>$ 130 deg FWZI
Eff. Area	$>$ 20 cm^2 @ 1 keV	$>$ 2 mm^2 @ 1 keV
Energy Res.	$<$ 150 eV @ 1 keV	$<$ 300 eV @ 6 keV
Energy Range	0.6−4 keV	1−8 keV
Timing Res.	$<$ 1 μs (SDD)	4 sec (histogram)

4 Mission Overview

The *LuXIS* spacecraft, weighing ∼43 kg in a $\sim 35 \times 23 \times 68$ cm volume, is designed to rideshare to the Moon as a secondary spacecraft during the next solar maximum. After insertion into an initial elliptical lunar orbit, *LuXIS* transfers to a science-optimized, low maintenance $\sim$ 6000 km quasi-frozen circular polar orbit ($\sim$ 17 hr period) for the 1-year science operation with a delta-V budget of $\sim$ 300 m/s. After the science orbit is reached, the quasi-frozen orbit requires relatively low maintenance, and will be stable enough without orbital maintenance to reach all primary science targets. During nominal science operations, 90% and 10% of the observation time is allocated to lunar XRF science and XNAV technology demonstration, respectively (e.g., Figure 5).

Unlike low lunar orbits ($\lesssim$100 km altitude) often employed for Lunar XRF measurements in the past, quazi-frozen high-altitude ($\gtrsim$6000 km) orbits enable long continuous monitoring of a handful of key targeted lunar sites with several hours spent in each orbit. With the ability to distinguish elemental composition with better than 3-km resolution within a ∼110-km FOV, *LuXIS* can address many questions of lunar evolution, including the identification of

outcrops of excavated mantle and lower crust material to probe magma ocean differentiation, studies of the vertical composition of near and farside crust, and exploration of volcanic domes and flows to understand the geochemical evolution of the mantle and crust.

Compared to the *Chandrayaan*/D-C1XS instrument (Grande et al., 2009), the reduced X-ray flux seen by the MiXO telescope due to the larger distance and the smaller FOV is largely compensated for by the larger effective area ($\gtrsim$20 cm^2), lower background ($\sim$100 times lower) and longer exposure ($\sim$100 times longer) for a given FoV footprint. A typical solar flare of any class lasts a few minutes to hours. A MiXO telescope in a high altitude orbit can monitor the same patch of the surface during the entire duration of a typical flare whereas D-C1XS cannot monitor the same patch for more than $\sim$20 sec with a FOV "footprint" of $\sim$25 km. By repeatedly viewing the same targets on each orbit, *LuXIS* can build up statistics for each, resulting in high-resolution elemental maps of scientifically important targets. Simulations indicate that with 500 ksec total integration, easily obtainable in a one-year mission, *LuXIS* can determine Mg/Si, Al/Si, Fe/Mg and other elemental ratios for six sites with relative precision ranging from 5% on a 100 km scale to 30% on a 3 km scale at C1 solar states, sufficient to distinguish diverse lunar compositions and address the science questions outlined above. A similar instrument flown on a full-scale lunar orbiter could do much, much more.

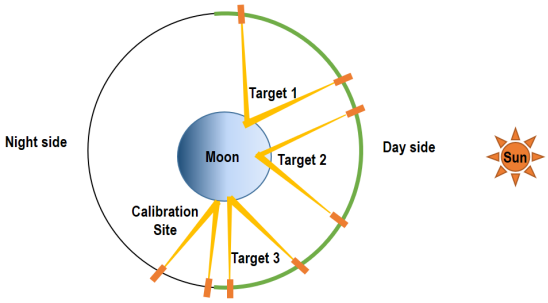

Figure 5: *Example XRF observing sequences for a noon-like orbit. The selected polar orbit changes from a noon-midnight orientation to terminator, and then back to a noon-midnight orientation over a 1-year science operation.*

5 Future Planetary X-ray Imaging Spectroscopy

LuXIS XIS's small form factor, low mass, and low power consumption (Table 1) open the door to a wide range of applications for various targets and missions including NEOs and Martian moons. A large number of low-cost *LuXIS* like S/C could revolutionize our understanding of NEOs and other airless bodies through rapid deployment to multiple targets.

References

Adler, I., et al., 1972, Science, 177, 256.
Adler, I., Schmadebeck, R., Trombka, J. I., Gorenstein, P., & Bjorkholm, P., 1975, Space Science Instrumentation, 1, 305.
Armytage, R. M. G., Georg, R. B., Williams, H. M., & Halliday, A. N., 2012, Geochimica et Cosmochimica Acta, 77, 504.
Chester, T. J., & Butman, S. A., 1981, Navigation using X-ray pulsars, Jet Propulsion Laboratory, Pasadena, CA, NASA Tech. Rep. 81N27129.
Clark, P. E., & Hawke, B., 1982, Lunar and Planetary Science Conference Proceedings, 12, 727.
Corley, L. M., McGovern, P. J., Kramer, G. Y., Lemelin, et al., 2018, Icarus, 300, 287.

Downs, G. S., 1974, Technical Report 32-1594 Interplanetary Navigation Using Pulsating Radio Sources (pp. 1-19) (United States of America, National Aeronautics and Space Ad- ministration). Pasadena, CA: Jet Propulsion Laboratory.
Elardo, S. M., Draper, D. S., & Shearer, C. K., 2011, Geochimica et Cosmochimica Acta, 75(11), 3024.
Fraser, G. W., et al., 2010, Planetary and Space Science, 58, 79.
Grande, M., et al., 2009, Planetary and Space Science, 57, 717.
Hong, J., Romaine, S., and the MiXO Team, 2016, Earth, Planets and Space, 68, 35.
Hong, J., Romaine, S., Nittler, L., Elvis, M., et al., 2020, X-ray Studies of Planetary Systems: A 2020 Decadal Survey White Paper, id.261.
Hong, J., Romaine, S., Nittler, L., Kring, D., et al., 2018, 49th Lunar and Planetary Science Conference, Woodlands, Texas, No. 2083, id.2793.
Jolliff, B. L., Wieczorek, M. A., Shearer, C. K., & Neal, C. R., 2006, New Views of the Moon, Reviews in Mineralogy and Geochemistry, Vol. 60. Mineralogical Society of America, Chantilly, VA.
Jolliff, B. L., Wiseman, S. A., Lawrence, S. J., Tran, T. N., Robinson, M. S., Sato, H., ... & Van Der Bogert, C. H., 2011, Nature Geoscience, 4(8), 566.
Kashyap, V. L., et al., 2020, Applied Optics, 59, 5560.
Kenter, A. T., Kraft, R., and Murray, S. S., 2012, SPIE, 8453, 84530G.
Kramer, G. Y., Kring, D. A., Nahm, A. L., & Pieters, C. M., 2013, Icarus, 223(1), 131.
Kramer, G. Y., Kring, D. A., Pieters, C. M., Head, J. W., et al., 2011, Lunar and Planetary Science Conference, 42, 1545.
Kring, D. A., Claeys, P., Gulick, S. P., Morgan, J. V., et al., 2017, Chicxulub and the Exploration of Large Peak-Ring Impact Craters through Scientific Drilling. GSA Today, 27(10).
Kring, D. A., Kramer, G. Y., Collins, G. S., Potter, R. W., & Chandnani, M., 2016, Nature communications, 7, 13161.
Lawrence, D. J., Feldman, W. C., Barraclough, B. L., Binder, A. B., et al., 1998, Science, 281(5382), 1484.
Lawrence, D. J., Feldman, W. C., Elphic, R. C., Little, R. C., et al., 2002, Journal of Geophysical Research: Planets, 107(E12).
Lemelin, M., Lucey, P. G., Song, E., & Taylor, G. J., 2015, Journal of Geophysical Research: Planets, 120(5), 869.
Melosh, H. J., Kendall, J., Johnson, B. C., Bowling, T., et al., 2014, Lunar and Planetary Science Conference, 45, 2505.
Papike, J., Taylor, L., & Simon, S., 1991, Lunar Minerals. In Lunar sourcebook: a user's guide to the Moon (pp. 121-182). Cambridge, England: Cambridge University Press.
Reichley, P., Downs, G., & Morris, G., 1971, JPL Quart. Tech. Rev, 1(2), 80.
Shearer, C. K., Burger, P. V., Bell, A. S., Guan, Y., & Neal, C. R., 2015, Meteoritics & Planetary Science, 50(8), 1449.
Smith, J. V., Anderson, A. T., Newton, R. C., Olsen, E. J., et al., 1970, Geochimica et Cosmochimica Acta Supplement, 1, 897.
Stupl, J., et al., 2018, 32nd Annual aIAA/USU Conference on Small Satellites, Logan, Utah, id 20180006866
Taylor, G. J., & Wieczorek, M. A., 2014, Phil. Trans. R. Soc. A, 372(2024), 20130242.
Vondrak, R., Keller, J., Chin, G., & Garvin, J., 2010, Space science reviews, 150(1-4), 7.
Warren, P. H., 2001, Geophysical research letters, 28(13), 2565.
Wieczorek, M. A., Neumann, G. A., Nimmo, F., Kiefer, W. S., et al., 2012, Science, 1231530.
Winternitz, L. M., Mitchell, J. W., Hassouneh, M. A., Valdez, J. E., et al., 2016, Aerospace Conference, IEEE, 1.
Witze, A., 2018, Nature 553, 261.
Wood, J. A. 1970, Journal of Geophysical Research, 75(32), 6497.
Wood, J. A., Dickey, J. S., Marvin, U. B., & Powell, B. N. 1970a, Science, 167(3918), 602.
Wood, J. A., Dickey Jr, J. S., Marvin, U. B., & Powell, B. N., 1970b, Geochimica et Cosmochimica Acta Supplement, 1, 965.
Yamamoto, S., Nakamura, R., Matsunaga, T., Ogawa, Y., et al., 2010, Nature Geoscience, 3(8), 533.
Yamamoto, S., Nakamura, R., Matsunaga, T., Ogawa, Y., et al., 2012, Icarus, 218(1), 331.